

# Interference of a Tonks-Girardeau Gas on a Ring

Kunal K. Das,<sup>\*</sup> G. John Lapeyre,<sup>†</sup> and Ewan M. Wright<sup>‡</sup>

*Optical Sciences Center and Department of Physics, University of Arizona, Tucson, AZ 85721*

(Dated: January 13, 2022)

We study the quantum dynamics of a one-dimensional gas of impenetrable bosons on a ring, and investigate the interference that results when an initially trapped gas localized on one side of the ring is released, split via an optical-dipole grating, and recombined on the other side of the ring. Large visibility interference fringes arise when the wavevector of the optical dipole grating is larger than the effective Fermi wavevector of the initial gas.

PACS numbers: 03.75.Fi, 03.75.-b, 05.30.Jp

## I. INTRODUCTION

Recently, theoretical arguments have been presented [1, 2] to demonstrate that several stimulated processes for matter waves such as four-wave mixing, superradiance and matter-wave amplification can be achieved in degenerate fermion gases as well as in Bose-condensed gases. Although such collective phenomena are often interpreted as characteristic of Bose-condensed systems, these theoretical studies show that this need not be the case. One of the earliest examples of matter-wave coherence was the demonstration of interference fringes in the density profile produced by colliding two Bose condensates (BECs) [3]. While it is true that the existence of off-diagonal long range order (ODLRO) in a system automatically implies first-order coherence, and density fringes may thus arise in a suitably designed interference experiment, this does not imply that if density fringes are observed the system under consideration automatically possesses ODLRO. In fact, such interference fringes can also arise for suitably prepared fermionic or thermal atom sources.

Our goal in this paper is to show that strong interference fringes can arise in a one-dimensional (1D) gas of impenetrable bosons, a Tonks-Girardeau (TG) gas, the conditions for which are essentially opposite from those required for BEC [4, 5], namely, the regime of low temperatures and densities and large positive scattering lengths where the transverse mode becomes frozen and the many-body Schrödinger dynamics becomes exactly soluble via a generalized Fermi-Bose mapping theorem [6, 7]. Even at zero temperature the TG gas does not display BEC into a single orbital, the condensate fraction varying as  $f \approx 1/\sqrt{N}$  for a system of  $N$  particles [8, 9]. The TG gas is therefore a good model system in which to study interference effects in non-condensed gases in 1D, which are currently of relevance due to experimental efforts to fabricate atomic waveguides for matter wave interferometers [10, 11]. Due to the intimate relation between the

TG gas and a gas of free fermions via the Fermi-Bose mapping our results also apply to the latter.

A simple model to study the dynamics of a TG gas is in a ring geometry which automatically imposes periodic boundary conditions. For the study of interference in 1D this geometry has the advantage that atomic wavepackets can be split and recombined without losing the strictly 1D nature of the system. In particular, we investigate the interference that results when an initially trapped gas localized on one side of the ring is released, split via an optical-dipole grating, and recombined on the other side of the ring. We study the dependence of the resulting interference fringes on various parameters such as the wavevector of the optical dipole grating and the number of atoms in the wavepacket.

The remainder of this paper is organized as follows: In Section II we set up our basic model, describe the Fermi-Bose mapping crucial for the description of a TG gas, and consider various conditions that need to be satisfied by our model for a consistent physical description. In section III we present numerical and analytic results for interference patterns and discuss experimental feasibility. Finally, we conclude with a discussion of the implications of our results and potential applications.

## II. BASIC MODEL FOR INTERFERENCE

In this section we describe our basic model of a TG gas on a ring, and describe our method of solving the quantum dynamics of the problem using the Fermi-Bose mapping.

### A. Tonks-Girardeau gas on a ring

The fundamental model we consider comprises of a 1D gas of  $N$  hard core bosonic atoms on a ring. This situation may be realized physically using a toroidal trap of high aspect ratio  $R = 2L/\ell_0$  where  $2L$  is the toroid circumference and  $\ell_0$  the transverse oscillator length  $\ell_0 = \sqrt{\hbar/m\omega_0}$  with  $\omega_0$  the frequency of transverse oscillations, assumed to be harmonic. The transverse trap potential is assumed to be radially symmetric about an axis consisting of a circle on which the trap potential

<sup>\*</sup>Electronic address: kdas@optics.arizona.edu

<sup>†</sup>Electronic address: Lapeyre@physics.arizona.edu

<sup>‡</sup>Electronic address: Ewan.Wright@optics.arizona.edu

is minimum. The longitudinal (circumferential) motion can be described by a 1D coordinate  $x$  along the ring with periodic boundary conditions applied. Then at zero temperature the quantum dynamics of the system is described by the time-dependent many-body Schrödinger equation (TDMBSE)  $i\hbar\partial\Psi_B/\partial t = \hat{H}\Psi_B$  with Hamiltonian

$$\hat{H} = -\frac{\hbar^2}{2m} \sum_{j=1}^N \frac{\partial^2}{\partial x_j^2} + V(x_1, \dots, x_N; t). \quad (1)$$

Here  $x_j$  is the 1D position of the  $j^{\text{th}}$  particle,  $\psi_B(x_1, \dots, x_N; t)$  is the  $N$ -particle wave function with periodic boundary conditions

$$\Psi_B(x_1, x_2, \dots, x_j + 2L, \dots, x_N) = \Psi_B(x_1, x_2, \dots, x_j, \dots, x_N), \quad (2)$$

which is also symmetric under exchange of any two particle coordinates in keeping with the Bose nature of the atoms, and the many-body potential  $V$  is symmetric (invariant) under permutations of the particles. The two-particle interaction potential is assumed to contain a hard core of 1D diameter  $a$ . This is conveniently treated as a constraint on allowed wave functions  $\Psi_B(x_1, \dots, x_N; t)$ :

$$\Psi_B = 0 \quad \text{if} \quad |x_j - x_k| < a, \quad 1 \leq j < k \leq N, \quad (3)$$

rather than as an infinite contribution to  $V$ , which then consists of all other (finite) interactions and external potentials. Here we explicitly consider the case  $a \rightarrow 0$  corresponding to a gas of impenetrable point bosons.

## B. Fermi-Bose mapping

To construct time-dependent many-boson solutions of Eq. (1) we employ the Fermi-Bose mapping [6, 12, 13] and start from fermionic solutions  $\Psi_F(x_1, \dots, x_N; t)$  on a ring of length  $2L$  of the TDMSE  $i\hbar\partial\Psi_F/\partial t = \hat{H}\Psi_F$  which are antisymmetric under all particle pair exchanges  $x_j \leftrightarrow x_k$ , hence all permutations. Next introduce a “unit antisymmetric function”

$$A(x_1, \dots, x_N) = \prod_{1 \leq j < k \leq N} \text{sgn}(x_k - x_j), \quad (4)$$

where  $\text{sgn}(x)$  is the algebraic sign of the coordinate difference  $x = x_k - x_j$ , i.e., it is  $+1(-1)$  if  $x > 0(x < 0)$ . For a given antisymmetric  $\Psi_F$ , define a bosonic wave function  $\Psi_B$  by

$$\Psi_B(x_1, \dots, x_N; t) = A(x_1, \dots, x_N) \Psi_F(x_1, \dots, x_N; t), \quad (5)$$

which defines the Fermi-Bose mapping. Then  $\Psi_B$  satisfies the hard core constraint (3) if  $\Psi_F$  does, is totally symmetric (bosonic) under permutations, and obeys the same boundary conditions [6, 7]. In the Olshanii limit [4] (low density, tight confined toroidal trap, large scattering length) the dynamics reduces to that of the impenetrable

point Bose gas, the  $a \rightarrow 0$  limit of Eq. (3). Then under the assumption that the many-body potential  $V$  of Eq. (1) is a sum of one-body external potentials  $V(x_j, t)$ , the solution of the fermion TDMBSE can be written as a Slater determinant [6, 13]

$$\Psi_F(x_1, \dots, x_N; t) = \frac{1}{\sqrt{N!}} \det_{(n,j)=(0,1)}^{(N-1,N)} \phi_n(x_j, t), \quad (6)$$

where the  $\phi_n$  are orthonormal solutions of the single particle time-dependent Schrödinger equation (TDSE)

$$i\hbar \frac{\partial \phi_n(x, t)}{\partial t} = \left[ -\frac{\hbar^2}{2m} \frac{\partial^2}{\partial x^2} + V(x, t) \right] \phi_n(x, t). \quad (7)$$

It then follows that  $\Psi_F$  satisfies the TDMBSE, and it satisfies the impenetrability constraint (vanishing when any  $x_j = x_\ell$ ) trivially due to antisymmetry. Then by the mapping theorem  $\Psi_B$  of Eq. (5) satisfies the same TDMBSE. The form of the single particle wavefunctions  $\phi_n(x, t)$  will depend on the choice of potential  $V(x, t)$ .

The utility of the Fermi-Bose mapping for the present problem of a TG gas lies in the fact that the density profiles for the Fermi and Bose problems are identical and are both obtained as a sum over the modulus squared of the orbitals obtained from Eq. (7)

$$\rho(x, t) = \sum_{n=0}^N |\phi_n(x, t)|^2. \quad (8)$$

This result follows from the fact that  $A^2(x_1, \dots, x_N) = 1$  and hence  $|\Psi_B|^2 = |\Psi_F|^2$ .

## C. Initial condition

For times  $t < 0$  the  $N$  atoms are confined to a narrow segment of the ring by a trapping potential  $V_{HO}(x)$  which is assumed harmonic with natural frequency  $\omega$  over the spatial extent of the initial trapped gas but drops off to zero beyond the confines of the trapped gas (to be consistent with the periodic boundary conditions the potential cannot be harmonic over the full ring). The basic configuration is shown schematically in Fig. 1(a). In order to later discuss the time-evolution of the system, it is convenient to designate the normal modes of an arbitrary 1D harmonic oscillator by its mean position  $\bar{x}$  and a parameter  $w$  that defines the width  $x_0\sqrt{1+w^2}$ :

$$u_n(x - \bar{x}, w) = \frac{C_n}{[1 + w^2]^{1/4}} e^{\frac{-(x - \bar{x})^2}{2(1 + w^2)x_0^2}} H_n \left[ \frac{x - \bar{x}}{\sqrt{1 + w^2} x_0} \right], \quad (9)$$

$$C_n = \frac{1}{\sqrt{\pi^{1/2} x_0 2^n n!}},$$

with  $H_n$  the Hermite polynomials and  $x_0 = \sqrt{\hbar/m\omega}$  the single-particle ground-state width corresponding to the initial trap potential  $V_{HO}(x)$ . Then the modes of the

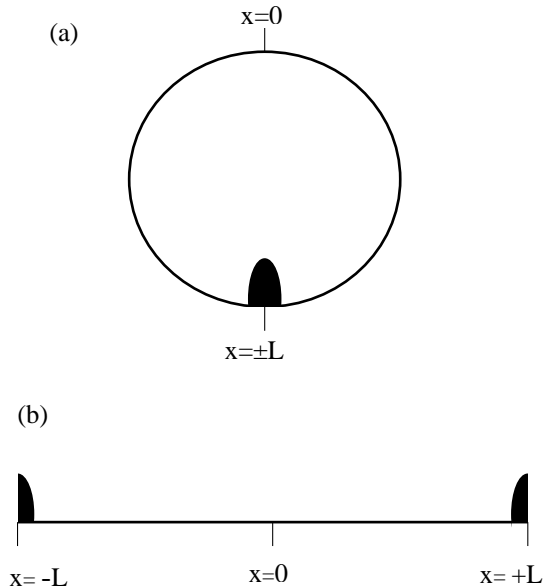


FIG. 1: (a) Our basic model consists of  $N$  hard core bosons trapped on a ring of circumference  $2L$ . (b) By unfolding the ring we describe the system using a 1D coordinate  $x \in [-L, L]$ . The coincident point  $x = -L \equiv L$  is chosen at the center of the initial trapped gas.

initial trap potential are given by  $u_n(x - \bar{x}, w = 0)$ , assuming that the trap is effectively harmonic for all modes  $n$  of interest. We choose our coordinates to have the trap center at  $x = L \equiv -L$ . On unwrapping the ring about  $x = 0$  in Fig. 1(b), the initial Hermite-Gaussian orbitals  $\phi(x, t < 0)$  are split into two parts at the ends of the interval  $[-L, L]$ , and can be written as

$$\phi_n(x, t \leq 0) = (-1)^n [u(x + L, 0) + u(x - L, 0)], \quad (10)$$

the factor of  $(-1)^n$  arising from the parity-reversal introduced by the unwrapping. The  $N$ -particle fermionic ground state  $\Psi_F^0$  has one particle in each of the  $N$  lowest levels [14], and the ground-state of the TG gas is given simply by  $\Psi_B^0 = |\Psi_F^0|$  [9], so the Fermi and TG gases have the same ground-state density profile. The width of the density profile of the  $N$ -particle ground state is  $x_N \approx \sqrt{2N} x_0$ . We want this initial state to be well localized on one side of the ring, which requires that  $L \gg x_N$  or

$$N \ll \frac{1}{2} \left( \frac{L}{x_0} \right)^2. \quad (11)$$

We also define an effective Fermi wavevector  $k_F$  for the initial state by examining the highest occupied mode  $n = N$ . For  $N \gg 1$  the asymptotic form of the Hermite polynomials yields  $\phi_N(x, 0) \propto \cos(\sqrt{2N}x)$  [15], which

corresponds to a highest occupied wavevector

$$k_F = \frac{\sqrt{2N}}{x_0}. \quad (12)$$

If the initial trapped gas is released at  $t = 0$  and left to expand freely it takes a time

$$t_{wrap} = \frac{L}{(\hbar k_F/m)} = \frac{1}{\omega \sqrt{2N}} \left( \frac{L}{x_0} \right), \quad (13)$$

for the highest excited orbital to start to wrap around the ring of length  $L$ . Equation (13) shows the explicit relation between the Fermi wavevector and the wrap time; the larger the atom number, and hence the Fermi wavevector, the shorter the wrap time.

Another time scale of physical significance is the Poincaré recurrence time  $t_{pr} = m(2L)^2/\pi\hbar = 4(L/x_0)^2/\pi\omega$ , which is the recurrence time for the density profile and all other physical quantities of the TG gas [12, 13]. Since we consider the limit  $L/x_0 \gg 1$  for a gas well localized on one side of the ring  $\omega t_{pr} \gg 1$ , and for this paper we consider times  $t \ll t_{pr}$  thereby prohibiting any recurrences.

A few conditions need to be satisfied for the TG gas to be realized on a ring. For the system to be frozen in a single transverse mode we require  $N\hbar\omega \ll \hbar\omega_0$ , with  $\omega_0$  the transverse oscillation frequency, or

$$N \ll \left( \frac{x_0}{\ell_0} \right)^2, \quad (14)$$

$\ell_0$  being the transverse ground-state width. Furthermore, for the initial gas to be accurately described as an impenetrable gas of bosons we require  $k_F|a_{1D}| \ll 1$ , where  $a_{1D}$  is the effective 1D scattering length [4]. From this condition we find

$$N \ll \frac{1}{2} \left( \frac{x_0}{a_{1D}} \right)^2 \simeq \frac{1}{2} \left( \frac{x_0 a}{\ell_0^2} \right)^2. \quad (15)$$

All three conditions in Eqs. (11), (14) and (15) need to be satisfied to realize a Tonks-Girardeau gas initially localized on one side of the ring.

#### D. Optical-dipole grating

In order to produce interference from the initial trapped gas we turn off the harmonic trap at  $t = 0$  and apply a temporally short but intense spatially periodic potential of wavevector  $k$ . This spatially periodic grating may be produced over the spatial extent of the trapped gas, for example, using intersecting and off-resonant pulsed laser beams to produce an intensity grating whose wavevector may be tuned by varying the intersection angle, which in turn produces a spatially periodic optical-dipole potential for the atoms. The applied periodic potential then produces counter-propagating scattered atomic waves, or daughter waves, from the initial

gas, or mother, with momenta  $\pm\hbar k$  and these recombine on the opposite side of the ring at a time

$$t_r = \frac{L}{(\hbar k/m)} = \left(\frac{k_F}{k}\right) t_{wrap}. \quad (16)$$

Clearly, if we want the scattered atoms to recombine before the initial gas wraps around the ring,  $t_r < t_{wrap}$ , we require  $k > k_F$ , otherwise interference of the scattered waves will be obscured by the wrapping.

The action of the optical dipole potential is best incorporated in our model before unwrapping with  $L \equiv -L$ , by writing the single-particle potential as a sum of the initial harmonic trap (HO) potential and the optical-dipole potential

$$V(x, t) = \theta(-t)V_{HO}(x) - \delta(t)\eta \cos[k(x - L)] e^{-\frac{(x-L)^2}{w^2}}, \quad (17)$$

where the Heaviside function  $\theta(-t)$  ensures that the harmonic trap turns off for  $t > 0$   $\eta$  is the strength of the applied periodic potential, and  $w$  is the spatial extent of the grating. In particular, the periodic grating due to the dipole potential need only extend over the spatial extent of the initial trapped gas,  $w > x_N$ , but we do require many periods of the grating  $kw \gg 1$ . For simplicity in presentation here we set  $w \rightarrow \infty$ . Furthermore, following Rojo *et. al.* [13] we have used a delta-function approximation for the short pulse excitation of the periodic grating at  $t = 0$ . Then by integrating Eq. (7) for each orbital over the delta-kick, just after the pulse at  $t = 0^+$  each Hermite-Gaussian mode is changed to

$$\begin{aligned} \phi_n(x, 0^+) &= e^{i\eta \cos[k(x-L)]} \phi_n(x, 0) \\ &= \sum_{m=-\infty}^{\infty} i^m J_m(\eta) e^{imk(x-L)} \phi_n(x, 0), \end{aligned} \quad (18)$$

where  $J_m$  are Bessel functions [15]. The subsequent quantum dynamics of the system is then traced by propagating each orbital  $\phi_n(x, 0^+)$  using Eq. (7).

For the present discussion we assume the limit  $|\eta| < 1$ , in which case

$$\phi_n(x, 0^+) \approx \left[1 + \frac{i\eta}{2} \left(e^{ik(x-L)} + e^{-ik(x-L)}\right)\right] \phi_n(x, 0), \quad (19)$$

and the optical-dipole grating predominantly produces two scattered waves with wavevectors  $\pm k$  in addition to the initial parent Hermite-Gaussian mode  $\phi_n(x, 0)$ . In particular, here we chose a value  $\eta = 1/2$  in which case 10% of the mother wave gets transferred into each daughter, and less than 1% is deflected into diffraction orders with  $|m| \geq 2$ . Note also that the daughter waves are simply reduced amplitude copies of the initial mode traveling to the left and right. We wish to examine the presence or absence of interference between the daughter waves at the opposite side of the ring at time  $t = t_r$  and how this depends on the wavevector  $k$  of the applied optical-dipole grating.

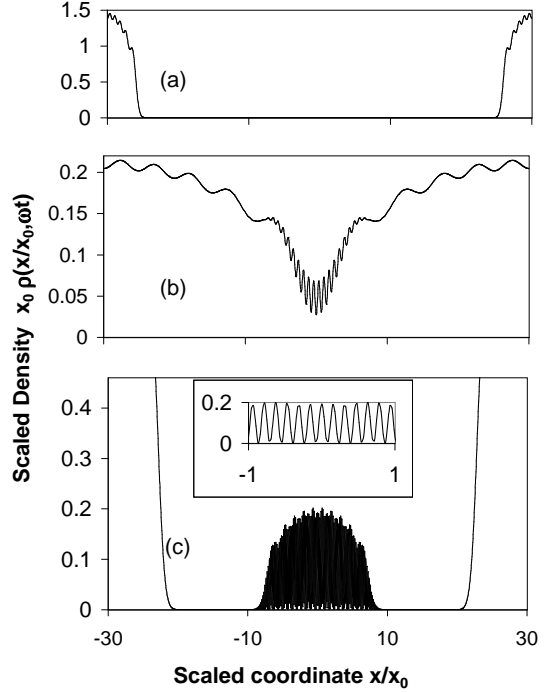


FIG. 2: Scaled density profiles  $x_0 \cdot \rho_B(x/x_0, \omega t)$  for  $N = 10$ ,  $\eta = 0.5$ ,  $L/x_0 = 30$  and (a) the initial condition  $t = 0$ , (b)  $x_0 k = 0$ ,  $\omega t = \omega t_{wrap} = 6.7$ , and (c)  $x_0 k = 20$ ,  $\omega t = \omega t_r = 1.5$ , the inset shows details of the fringes.

### III. INTERFERENCE ON A RING

#### A. Numerical simulations

To set the stage for the analytic results below, Fig. 2 shows illustrative examples of interference on a ring for  $N = 10$  atoms under various conditions. To produce numerical results we solve the Schrödinger equation (7) for each orbital with the initial condition (18) using the split-step Fast-Fourier transform method [16], and calculate the density using Eq. 8 for the density. Figure 2 shows the scaled density profiles  $x_0 \cdot \rho_B(x/x_0, \omega t)$  for  $\eta = 0.5$ ,  $L/x_0 = 30$  and (a) the initial condition  $t = 0$ , (b)  $x_0 k = 0$ ,  $\omega t = \omega t_{wrap} = 6.7$ , and (c)  $x_0 k = 20$ ,  $\omega t = \omega t_r = 1.5$ . Note that the initial density profile in Fig. 2(a) appears split due to the choice of origin in Fig. (1). In Fig. 2(b) we have allowed the initial trapped gas to expand freely ( $k = 0$  is equivalent to no grating at all) and the density is plotted at a time equal to the wrap time  $\omega t_{wrap} = 6.7$ . Here we see that while there is some degree of interference the visibility is not very large, and we show in the next subsection that these fringes tend to vanish for large numbers of atoms. In contrast, mean-field theory, in which

the matter waves are described by a single orbital obeying a nonlinear Schrödinger equation, results in a visibility close to unity. (We discussed the failure of mean-field theory for TG gases elsewhere in our previous paper [17]). By comparison Fig. 2(c) for  $x_0 k = 20, \omega t = \omega t_r = 1.5$  shows very clean interference fringes in the density with wavevector  $k_{int} = 2k$  between the scattered waves upon recombination at  $t = t_r$  with almost unity visibility. As we show below, these fringes do not vanish in the limit of large  $N$  as long as  $k > k_F$  is maintained.

These numerical simulations highlight our main findings: First, for  $k/k_F \ll 1$  at best low visibility interference fringes are seen, and this clearly results from the fact that the initial trapped gas has now wrapped around the ring at  $t = t_r > t_{wrap}$ . Second, for  $k/k_F \gg 1$  large visibility interference fringes between the recombined scattered waves can be observed. Rojo *et. al.* [13] obtained the same criterion for the appearance of Talbot oscillations in a 1D TG gas on a ring of size  $L$ . In their case the initial state of the gas is homogeneous on the ring with no external trap, for which  $k_F = \pi N/L$ , and the Talbot oscillations in the density due to the applied grating are undamped only for  $k/k_F \gg 1$ .

## B. Analytic results

In this section we develop an analytic approach to describe the interference fringes for the TG gas on a ring. Immediately after the periodic potential is applied and the harmonic trap turned off, the single particle modes (19) for the atoms in the unwrapped configuration assume the form

$$\phi_n(x, 0^+) \approx (-1)^n \left[ \left( 1 + \frac{i\eta}{2} e^{ik(x+L)} \right) u_n(x+L, 0) + \left( 1 + \frac{i\eta}{2} e^{-ik(x-L)} \right) u_n(x-L, 0) \right]. \quad (20)$$

For each  $n$  this initial condition is the same as a superposition of waves centered at  $x = \pm L$  on the infinite line  $x \in [-\infty, \infty]$  since the initial gas is well localized on one side of the ring. The evolution of each orbital  $\phi_n(x, t)$  may therefore be approximated as free propagation on the infinite line for times  $t < \min(2t_r, 2t_{wrap})$ . For example, for the case of no applied optical dipole potential  $\eta = 0$ , at  $t = t_{wrap}$  the tails of the two expanding packets start to overlap at  $x = 0$  corresponding to wrapping of the mother packet, whereas at  $t = 2t_{wrap}$  the tails of the expanding packets start to circle back to  $x = L \equiv -L$ . Therefore, for  $t \geq 2t_{wrap}$  the solution has spread over the full ring, and approximation of the evolution of the orbitals as free expansion on the infinite line is no longer valid.

Here we use the approximation of free expansion of the orbitals to investigate the interference fringes at  $t = t_r$  and  $t = t_{wrap}$ . Then the total particle density anywhere along the ring for  $t > 0$  retains the simple structure

shown in Eq. (8) i.e. it is simply the sum of the densities due to each occupied mode. Each initial wavefunction  $\phi_n(x, 0^+)$  in Eq. (20) may be separately evolved for  $t > 0$  using the retarded free-particle Green's function to obtain

$$\phi_n(x, t) = \frac{1}{\sqrt{2\pi i \omega t}} \int_{-\infty}^{\infty} dx' \phi_n(x', 0^+) e^{-\frac{(x-x')^2}{2i\omega t}}. \quad (21)$$

Due to the symmetric form of the initial wavepacket the centers of the daughter packets arrive at  $x = 0$  simultaneously at a time  $t_r$  given by Eq. (16). The time-evolved functions can be written in terms of the functions  $u_n(x - \bar{x}, w)$  defined in Eq. (9). At  $t = t_r$  the daughter components are centered at  $x = 0$  and their width increased to  $x_0 \sqrt{1 + \omega^2 t_r^2}$ , thus their moduli are identical and given by  $u_n(x, \omega t_r)$  but their phases are different due to opposite velocities and the fact that the time-evolved modes acquire a spatial phase variation as they expand. The mother packet has the same increase in width but is still centered at  $x = \pm L$  and hence its two ends have moduli given by  $u_n(x \pm L, \omega t_r)$  and their phases, being space-dependent, are different as well.

On using the time-evolved wavefunctions  $\phi_n(x, t_r)$  in Eq. (8) we obtain an analytic expression for the density of atoms in the neighborhood of  $x = 0$  which comprises three distinct contributions

$$\rho(x, t_r) = \rho_m(x, t_r) + \rho_d(x, t_r) + \rho_{md}(x, t_r). \quad (22)$$

The first term is due to the freely expanding mother packet overlapping with itself

$$\rho_m(x, t_r) = \sum_{n=0}^{N-1} [u_n^2(x+L, \omega t_r) + u_n^2(x-L, \omega t_r) + 2u_n(x+L, \omega t_r)u_n(x-L, \omega t_r) \cos(2Qx)]. \quad (23)$$

with a mode-independent sinusoidal modulation of period  $\pi/Q(t_r) = \pi x_0^2(1 + \omega^2 t_r^2)/L\omega t_r$  which arises from the spatial phase variation developed by the expanding mode functions. This would be the sole contribution if  $\eta = 0$  i.e. in the absence of any daughter packets. Figure 3 shows that the visibility of the fringes arising from the mother packet wrapping around the ring diminishes with increasing number of particles. The reason for this is apparent from the above expression for  $\rho_m$ , namely, while the first two terms representing the background being the modulus squared of the orbitals are positive definite for all values of  $n$ , for a given  $n$  the sign of the product of Hermite-Gaussians  $u_n(x+L, \omega t_r)u_n(x-L, \omega t_r)$  in the cross term responsible for the interference fringes can have either sign. Thus, upon summing over  $n$  the value of the cross term is in general degraded by cancellations with respect to the background terms in Eq. (23). For larger number of particles  $N$  the Hermite polynomials become more oscillatory spatially [15] and we expect the cancellations to become more complete, while the background increases like  $N$ , hence the fringe contrast due to wrapping of the mother packet decreases with  $N$ . This physical picture of the degradation of the density interference

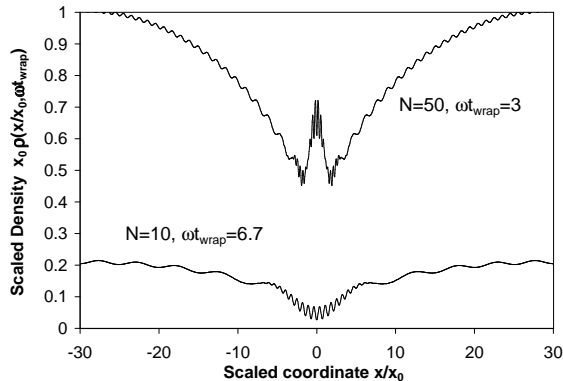


FIG. 3: Scaled density profiles at  $t_{wrap}$  for  $\eta = 0$  using the analytic expression in Eq. (23). It shows that for a larger particle number  $N$  there is lower visibility of the fringes due to the overlap of the expanding mother packet with itself.

fringes due to destructive interference of orbitals is in agreement with our previous discussion of the failure of mean-field theory for a TG gas [17], that is, the quantum dynamics of a TG gas cannot be correctly captured by a single orbital, though Kolomeisky *et al.* [14] have shown that mean-field theory can yield the ground state density profile.

The second term arises from the complete overlap of the daughter packets at the recombination time  $t_r$

$$\rho_d(x, t_r) = \frac{\eta^2}{2} [1 + \cos(2kx)] \sum_{n=0}^{N-1} u_n^2(x, \omega t_r). \quad (24)$$

In the case when  $k \gg k_F$  this term dominates in the vicinity of  $x = 0$  at  $t_r$  and produces fringes of essentially unit visibility, and the amplitude of the modulation would increase with particle number. This explains the strong fringes seen in Fig. 2 (c) discussed in the previous section. The form of the interference pattern (24) is identical to that obtained by Moore and Meystre [1] for a Fermi gas exposed to a Bragg grating, and verifies within the context of an exactly soluble model that both the TG and Fermi gases can exhibit high visibility interference fringes.

For  $k$  comparable or smaller than  $k_f$  the clean fringes are lost. This is mainly due to the background introduced by the mother packet overlapping with itself. There is also a more complicated modulation due to the overlap of the daughter packets with the mother packet given by

$$\rho_{md}(x, t_r) = -2\eta \cos(kx) \sum_{n=0}^{N-1} u_n(x, \omega t_r) \times [u_n(x-L, \omega t_r) \sin(\phi+Qx) + u_n(x+L, \omega t_r) \sin(\phi-Qx)] \quad (25)$$

The sinusoidal modulation here has twice the period as that of  $\rho_m$  and in addition there is a time-dependent

phase  $\phi(t_r) = Lk/2(1+\omega^2 t_r^2)$ . For our choice of the point of detection, diametrically opposite the center of the initial packet, the relative importance of this contribution diminishes with increasing particle number. This is because in the neighborhood of  $x = 0$ ,  $u_n(x)u_n(x \pm L) < u_n^2(x)$  and this difference is enhanced as more modes are included in the sum. Thus for a large number of particles the density distribution around  $x = 0$  at time  $t_r$  can be well described by the full visibility modulation arising from the interference of the daughters superimposed on the background density due to each end of the expanding initial packet.

### C. Experimental feasibility

Although it is not yet possible to realize a TG gas on a ring it is of interest to examine some parameters to assess the possibility of experimental realization. Let us first consider the conditions required to achieve the impenetrable TG regime. Among the two constraints on the number of particles in Eq. (14) and (15), the second one is more limiting since a positive 1D scattering length requires  $\ell_0 > a$  [4]. For sodium atoms with scattering length  $a=2.75$  nm this limits the number of particles to  $N \ll 10^{-8} \times (\nu_0^2/\nu)$  where  $\omega_0 = 2\pi\nu_0$ . A choice of  $\nu \sim 1$  Hz for a weak longitudinal confinement would mean that for  $N=100$  atoms we would still need in excess of  $10^5$  Hz transverse confinement frequency, which is about two orders of magnitude above the limits of current experimental trap frequencies. We also note that for the atoms in the daughter packets to remain impenetrable the transverse potential should also be tight enough to satisfy  $k|a_{1D}| \ll 1$  which is relevant for momentum kicks  $k > k_F$  needed to observe clean fringes.

For  $\nu \sim 1$  Hz the oscillator length is  $x_0 \sim 10^{-5}$  m and hence  $k_F \sim \sqrt{N} \times 10^5 \text{ m}^{-1}$ . The wavevectors corresponding to the yellow sodium lines are about  $k \sim 10^7 \text{ m}^{-1}$ , thus the maximum boosts we can realistically consider are about  $k/k_F \sim 100/\sqrt{N}$ . The values of  $k$  we used for our plots satisfy this condition. Corresponding to this oscillator length the condition for a well localized initial packet stated in Eq. (11) will require a ring size of  $2L \sim 1$  mm, an experimentally realistic size for atom interferometers.

At the same time, while the TG limit is very interesting it is not a requirement for observation of interference fringes in the ring configuration: Even if the atoms are penetrable, interference of the scattered waves is expected anyway. If we have a dilute gas of fermions instead of bosons we need only satisfy constraint Eq. (14) for 1D behavior which requires the much weaker constraint  $N \ll \nu_\perp/\nu$ . Even with currently achievable trap conditions it should be possible to realize up to  $N \sim 1000$  fermionic atoms in the ring configuration and produce interference fringes. Actual observation of the fringes however might be difficult due to the low atom number.

#### IV. SUMMARY AND CONCLUSIONS

In conclusion, we have shown that a Tonks-Girardeau gas on a ring can show large visibility interference fringes. This demonstrates in the framework of the exactly soluble many-body TG gas problem that one does not need a BEC or a source possessing high-order coherence to get interference fringes in principle. Physically, the reason interference fringes can appear even for an incoherent atom source is that the optical dipole grating imprints a different spatially dependent phase on each of the diffracted fragments and the interference fringe seen from subsequent recombination of those fragments reflects the effect of the imprinted phase rather than the intrinsic coherence of the initial or mother packet. Furthermore, if the ring is rotating, the interference fringes due to interference of the daughter waves will shift due to the Sagnac effect: This is easily deduced by realizing that the usual Sagnac

effect will apply to each individual orbital independent of orbital number. This implies in turn that rotation sensors, in principle, also do not require a coherent source of atoms.

In addition to the large visibility fringes that result from interference of daughter waves that survive in the limit of large  $N$ , fringes can also appear due to the wrapping of the mother wave around the ring. However, the visibility of the fringes due to wrapping was shown to decrease with increasing particle number, thereby vanishing in the thermodynamic limit.

We appreciate valuable discussions with Professor Marvin Girardeau of the Optical Sciences Center, University of Arizona, and Prof. Mara Prentiss of Harvard University. This work was supported by the Office of Naval Research Contract No. N00014-99-1-0806, and the U.S. Army Research Office.

- 
- [1] M. G. Moore and P. Meystre, *Phys. Rev. Lett.* **86**, 4199 (2001).
  - [2] Wolfgang Ketterle and Shin Inouye, *Phys. Rev. Lett.* **86**, 4203 (2001).
  - [3] M. R. Andrews *et al.*, *Science* **275**, 637 (1997).
  - [4] M. Olshanii, *Phys. Rev. Lett.* **81**, 938 (1998).
  - [5] D.S. Petrov *et al.*, *Phys. Rev. Lett.* **85**, 3745 (2000).
  - [6] M. Girardeau, *J. Math. Phys.* **1**, 516 (1960).
  - [7] M.D. Girardeau, *Phys. Rev.* **139**, B500 (1965). See particularly Secs. 2, 3, and 6.
  - [8] A. Lenard, *J. Math. Phys.* **7**, 1268 (1966).
  - [9] M.D. Girardeau, E.M. Wright, and J. M. Triscari, *Phys. Rev. A* **63**, 033601 (2001).
  - [10] E. A. Hinds *et al.*, *Phys. Rev. Lett.* **80**, 645 (1998); J. Schmiedmayer, *Eur. Phys. J. D* **4**, 57 (1998); M. Key *et al.*, *Phys. Rev. Lett.* **84**, 1371 (2000); D. Müller *et al.*, physics/9908031.
  - [11] J. H. Thywissen *et al.*, *Eur. Phys. J. D* **4**, 57 (1998); *Phys. Rev. Lett.* **83**, 3762 (1999); *Eur. Phys. J. D* **7**, 261 (1999).
  - [12] M.D. Girardeau and E.M. Wright, *Phys. Rev. Lett.* **84**, 5691 (2000).
  - [13] A. G. Rojo, G. L. Cohen, and P. R. Berman, *Phys. Rev. A* **60**, 1482 (1999).
  - [14] E. B. Kolomeisky, T. J. Newman, J. P. Straley, and Xiaoya Qi, *Phys. Rev. Lett.* **85**, 1146 (2000).
  - [15] I. S. Gradshteyn and I. M. Ryzhik, *Table of Integrals, Series and Products, Fifth Edition* (Academic Press, London, 1994).
  - [16] J. A. Fleck, J. R. Morris, and M. D. Feit, *Appl. Opt.* **10**, 129 (1976).
  - [17] M.D. Girardeau and E.M. Wright, *Phys. Rev. Lett.* **84**, 5239 (2000).